Transcription factor Runx2 controls the development and migration of plasmacytoid dendritic cells

Catherine M. Sawai,[1] Vanja Sisirak,[1] Hiyaa S. Ghosh,[1] Esther Z. Hou,[1] Michele Ceribelli,[2] Louis M. Staudt,[2] and Boris Reizis[1]

[1]Department of Microbiology and Immunology, Columbia University Medical Center, New York, NY 10032
[2]Metabolism Branch, Center for Cancer Research, National Cancer Institute, National Institutes of Health, Bethesda, MD 20892

Plasmacytoid dendritic cells (pDCs) rapidly produce type I interferon (IFN-I) in response to viruses and are essential for antiviral immune responses. Although related to classical DCs (cDCs) in their development and expression profile, pDCs possess many distinct features. Unlike cDCs, pDCs develop in the bone marrow (BM) and emerge into peripheral lymphoid organs and tissues as fully differentiated cells. We now report that pDCs specifically express Runx2, a Runt family transcription factor that is essential for bone development. pDCs in Runx2-deficient mice developed normally in the BM but were greatly reduced in the periphery. The defect was cell-intrinsic and was associated with the retention of mature Ly49Q$^+$ pDCs in the BM. Runx2 was required for the expression of several pDC-enriched genes, including the chemokine receptors Ccr2 and Ccr5. Mature pDCs expressed high levels of Ccr5 at the cell surface, and Ccr5-deficient pDCs in a competitive setting were reduced in the periphery relative to the BM. Thus, Runx2 is required for the emergence of mature BM pDCs into the periphery, in a process that is partially dependent on Ccr5. These results establish Runx2 as a lineage-specific regulator of immune system development.

CORRESPONDENCE
Boris Reizis:
bvr2101@columbia.edu

Abbreviations used: cDC, classical DC; ChIP, chromatin immunoprecipitation; Dox, doxycycline; pDC, plasmacytoid DC; shRNA, short hairpin RNA.

Plasmacytoid DCs (pDCs) comprise a unique immune cell type dedicated to the production of key antiviral cytokines, type I IFNs (IFN-α/β, IFN-I). pDCs detect viral nucleic acids through the endosomal TLRs TLR7 and TLR9, as well as through cytoplasmic sensors. The activation of these sensing pathways in pDCs leads to IFN-I secretion that is much more rapid and abundant than in other cell types (Colonna et al., 2004; Reizis et al., 2011). This unique capacity of pDCs for IFN-I production is facilitated by multiple adaptations, such as secretory morphology, high levels of IFN-activating transcription factor IRF7, and the expression of pDC-specific adaptors such as Pacsin1 (Bao and Liu, 2013). The pDC-derived IFN-I protects cells against viruses and activates multiple immune cell types, establishing pDCs as a key link between innate and adaptive immunity. Indeed, pDCs are required for IFN-I response and innate defense against several acute viral infections, as well as for adaptive T cell response against persistent viral infections (Swiecki et al., 2010; Cervantes-Barragan et al., 2012). Conversely, aberrant IFN-I production by pDCs has been implicated in the progression of several autoimmune diseases, such as lupus and psoriasis.

The analysis of pDC development, regulation, and gene expression profile firmly established their close relationship with classical or conventional DCs (cDCs; Reizis et al., 2011). Both pDC and cDC lineages develop in the BM from a common DC progenitor and are dependent on the growth factor Flt3 ligand (Flt3L; Liu and Nussenzweig, 2010). However, the development and homeostasis of committed pDCs differ from those of cDCs in several important aspects. Whereas committed cDC progenitors exit the BM and differentiate in the periphery, pDCs undergo full differentiation in the BM. Functional differentiation of murine pDCs is accompanied by the acquisition of pDC-specific receptor Ly49Q (Kamogawa-Schifter

The Rockefeller University Press $30.00
J. Exp. Med. 2013 Vol. 210 No. 11 2151-2159
www.jem.org/cgi/doi/10.1084/jem.20130443

The Journal of Experimental Medicine

et al., 2005; Omatsu et al., 2005), which is required for optimal IFN-I production (Tai et al., 2008). Mature Ly49Q$^+$ pDCs exit the BM and home through blood to peripheral lymphoid organs, unlike cDCs that migrate through afferent lymphatics. Steady-state migration of pDCs into specific tissues is controlled by chemokine receptors such as Ccr7 and Ccr9, which facilitate pDC entrance into the LNs and gut, respectively (Wendland et al., 2007; Seth et al., 2011). The activation of pDCs by viruses or TLR ligands changes their homing pattern, including enhanced migration to the LN and clustering in the spleen (Asselin-Paturel et al., 2005; Diacovo et al., 2005). However, little is known about the lineage-specific mechanisms that regulate pDC migration in the steady state, including exit from the BM into the periphery.

The development of pDCs is controlled by several transcription factors, including common regulators of DC lineage such as Stat3, PU.1, and Irf8 (Miller et al., 2012; Satpathy et al., 2011). The specification of pDC lineage depends on E protein transcription factor E2-2 (Tcf4), which is preferentially expressed in murine and human pDCs (Cisse et al., 2008). The deletion of E2-2 completely abolishes pDC development but does not affect any other immune cell type. E2-2 directly controls the conserved expression program of pDCs, including key functional genes such as *TLR9*, *PACSIN1*, and *IRF7* (Ghosh et al., 2010). One of the major targets of E2-2 is *SPIB*, which encodes a transcription factor preferentially expressed in pDCs and B lymphocytes. Recently, it has been shown that SpiB regulates the transition from immature Ly49Q$^-$ to mature Ly49Q$^+$ pDCs in the murine BM. The loss of SpiB caused premature exit of Ly49Q$^-$ pDCs from the BM into the periphery, where they showed defective IFN-I responses (Sasaki et al., 2012). Thus, pDC development and homeostasis are mediated by a lineage-specific network of transcription factors orchestrated by E2-2. However, pDC-specific transcription factors that regulate late differentiation steps including the migration of mature pDCs remain unknown.

The Runx family of transcription factors in vertebrates consists of three proteins (Runx1-3) that are orthologous to the Runt protein of *Drosophila melanogaster*. These proteins form heterodimers with the common subunit CBFβ to regulate the transcription of target genes. Runx1 and Runx3 have been extensively studied within the hematopoietic system, where they often act as repressors that direct cell fate choices. In particular, Runx1 and Runx3 are critical regulators of T cell differentiation, including the choice between CD4 and CD8 T cell lineages and effector T cell differentiation pathways (Collins et al., 2009). On the other hand, Runx2 is known as a master regulator of bone development, where it acts primarily as an activator to facilitate the generation of osteoblasts and subsequent bone formation (Long, 2012). To date, the role of Runx2 within the hematopoietic system has not been explored.

We now report that Runx2 is expressed specifically in pDCs in an E2-2–dependent manner, and is required for pDC migration from the BM into the periphery. We also identify chemokine receptor Ccr5 as a Runx2-dependent gene that facilitates pDC homing to peripheral lymphoid organs. These data establish a cell-intrinsic role of Runx2 in immune system development, and elucidate a novel transcriptional regulator of pDC development and homeostasis.

RESULTS AND DISCUSSION

Runx2 is a target of E2-2 and is expressed specifically in pDCs

To identify additional regulators of pDC development, we searched for transcription factors whose expression is directly activated by E2-2 in pDCs. The expression of *RUNX2* has been previously detected by microarrays in human pDC-derived lymphomas (Dijkman et al., 2007), including the human pDC cell line CAL-1 (Cisse et al., 2008). Chromatin immunoprecipitation/deep sequencing (ChIP-Seq) analysis of E2-2 target genes in CAL-1 cells showed prominent E2-2 binding to the *RUNX2* locus. In addition to several major binding peaks in the intron and 3′ region, the binding of E2-2 to *RUNX2* promoter was also detected (Fig. 1 A). After doxycycline (Dox)-inducible knockdown of E2-2 by short hairpin RNA (shRNA), we observed a reduction in *RUNX2* expression in CAL-1 (unpublished data) as well as in another human pDC cell line, Gen2.2 (Fig. 1 B). The reduction was comparable to that of *TCF4* (the gene encoding E2-2) itself; in contrast, another direct E2-2 target SLA2 (Ghosh et al., 2010) did not decrease in these conditions. These results suggest that *RUNX2* is directly activated by E2-2 in human pDCs.

In the mouse, preferential expression of *Runx2* in sorted pDCs compared with cDCs has been noticed in microarray-based expression studies (Crozat et al., 2010; Satpathy et al., 2011; Miller et al., 2012). To analyze *Runx2* expression in the entire hematopoietic system at the single-cell level, we used *Runx2* allele with the LacZ reporter replacing the first coding exon (Otto et al., 1997). The analysis of LacZ expression in *Runx2*$^{LacZ/+}$ heterozygous (Het) mice by flow cytometry showed a specific LacZ$^+$ population in the BM (Fig. 1 C) and peripheral lymphoid organs (not depicted). Almost all LacZ$^+$ cells showed the Bst2$^+$ B220$^+$ phenotype characteristic of pDCs (Fig. 1 C). Conversely, only pDCs but no other lineages (including cDCs or B cells) harbored a LacZ$^+$ population in the BM, spleen, and LN (Fig. 1, D and E). The partial expression of LacZ in pDCs likely reflects the variegation of the reporter allele, which includes the heterologous drug selection cassette. Indeed, the expression of the wild-type *Runx2* allele was comparable in LacZ$^+$ and LacZ$^-$ populations (not depicted), and *Runx2*$^{LacZ/LacZ}$ pDCs showed a more uniform LacZ expression (Fig. 1 E). Collectively, these data demonstrate that within the hematopoietic system, *Runx2* is expressed specifically in the pDC lineage.

Runx2 is required for the exit of mature pDCs from the BM

To determine the functional significance of Runx2 expression in pDCs, we analyzed homozygous *Runx2*$^{LacZ/LacZ}$ KO cells. Because KO mice die perinatally due to failed ossification, we reconstituted irradiated CD45.1$^+$ recipient mice with KO or control WT fetal liver cells. Flt3L-supplemented cultures of

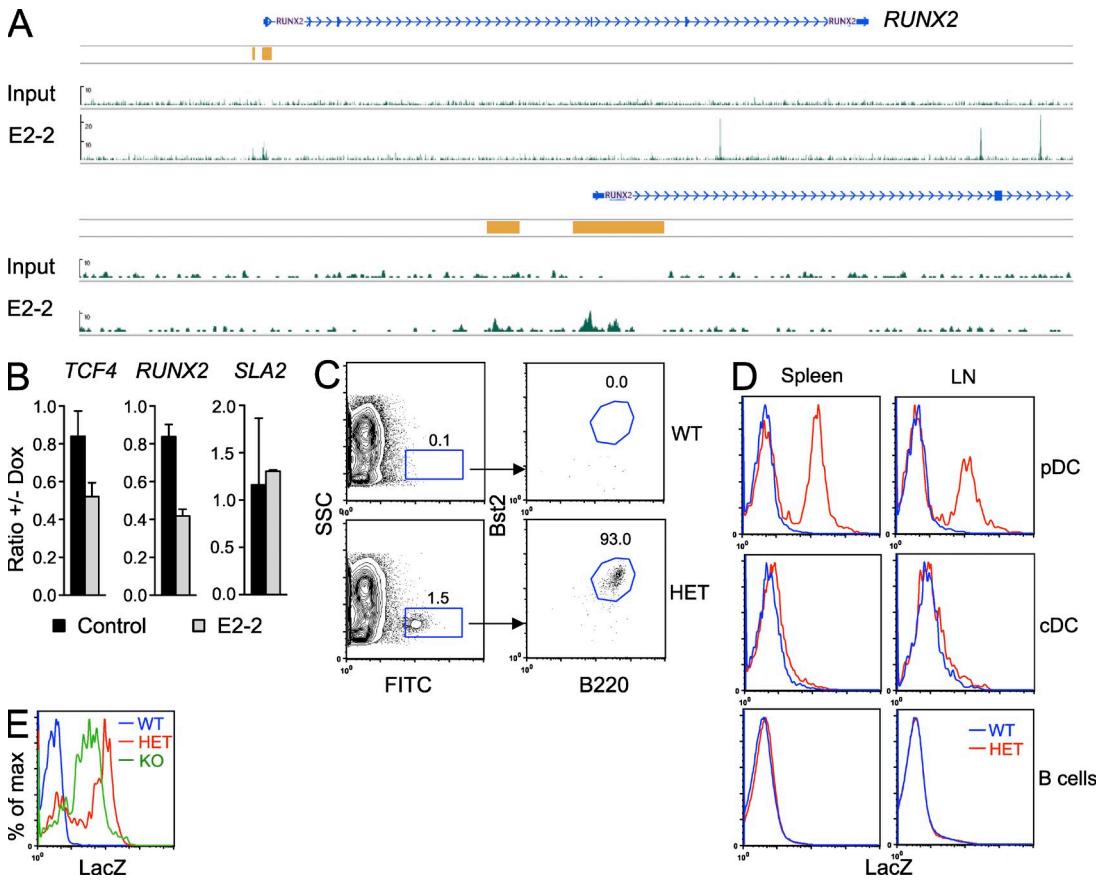

Figure 1. ***Runx2*** **is a direct target of E2-2 and is specifically expressed in pDCs.** (A) Enrichment peaks of E2-2 ChIP or total chromatin from the human pDC cell line CAL-1 across the entire *RUNX2* locus (top) and its promoter region (bottom). The CpG island at the promoter is shown in orange. (B) Cells of the human pDC cell line Gen2.2 were treated with Dox to induce the expression of E2-2–specific or scrambled control shRNAs. The expression of *TCF4* (the gene encoding E2-2) and E2-2–binding targets *RUNX2* and *SLA2* was measured by qRT-PCR. Shown is the ratio of expression levels with or without Dox (mean ± SD of triplicate reactions). (C) BM cells from $Runx2^{LacZ}$ reporter mice were stained for LacZ by flow cytometry to analyze the expression of Runx2. (left) Total BM cells from control WT or heterozygous (Het) $Runx2^{LacZ/+}$ mice. (right) The gated LacZ$^+$ population stained for pDC markers Bst2 and B220. (D) Gated pDC (CD11b$^-$ B220$^+$ Bst2$^+$), cDC (CD11c^{hi} MHC II$^+$), and B cell (CD11c$^-$ B220$^+$) populations from the spleens and LN of WT and Het mice were analyzed for the expression of LacZ by flow cytometry. (E) Donor-derived pDCs (CD45.2$^+$ B220$^+$ Bst2$^+$) from recipient mice reconstituted with WT, Het, or homozygous KO $Runx2^{LacZ/LacZ}$ cells were analyzed for LacZ expression.

BM cells from the resulting chimeric mice showed normal development of KO pDCs (unpublished data). Within the BM, the fraction of KO donor-derived CD45.2$^+$ Bst2$^+$ B220$^+$ pDCs was slightly but significantly increased compared with WT-derived pDCs (Fig. 2, A and B). In contrast, the frequencies of KO pDCs were reduced 4–5-fold in the peripheral blood, spleen, and LNs (Fig. 2, A and B). A comparable decrease was also observed in the very small fraction of pDCs in the thymus (Fig. 2 B). On the other hand, no significant pDC decrease was detected in the Peyer's patches, which support a divergent IFN-dependent pathway of pDC development (Li et al., 2011). Thus, all populations of BM-derived peripheral pDCs were decreased in KO chimeras, whereas the pDC population that may develop in situ was less affected. The decrease was restricted to pDCs, as other hematopoietic populations were detected at normal percentages in the spleen and LN (Fig. 2 C). Furthermore, serum IFN-α production in response to TLR9 ligand unmethylated CpG oligonucleotide (CpG) was severely impaired in mice reconstituted with KO cells (Fig. 2 D). Because CpG-induced IFN-α production is completely dependent on pDCs (Cisse et al., 2008), these data confirm the loss of peripheral pDCs after Runx2 deletion.

Next, we generated competitive chimeras in which WT or KO fetal liver cells were mixed at a 1:1 ratio with CD45.1$^+$ total BM cells and transplanted into irradiated CD45.1$^+$ recipients. The fractions of donor-derived CD45.2$^+$ pDCs in the BM were comparable between recipients of WT and KO cells; however, the fraction of KO pDCs was strongly reduced in the spleen (Fig. 2 E). We also determined the ratios of donor-derived CD45.2$^+$ to competitor-derived CD45.1$^+$ cells in each immune lineage, and normalized the ratios from the spleen and LN to those in the BM. We found that the ratio of donor to competitor pDCs was decreased >6-fold in the spleen and LN of KO cell recipients (Fig. 2 F). This defect was specific to pDCs, because other KO hematopoietic lineages including B and T cells and granulocytes were detected

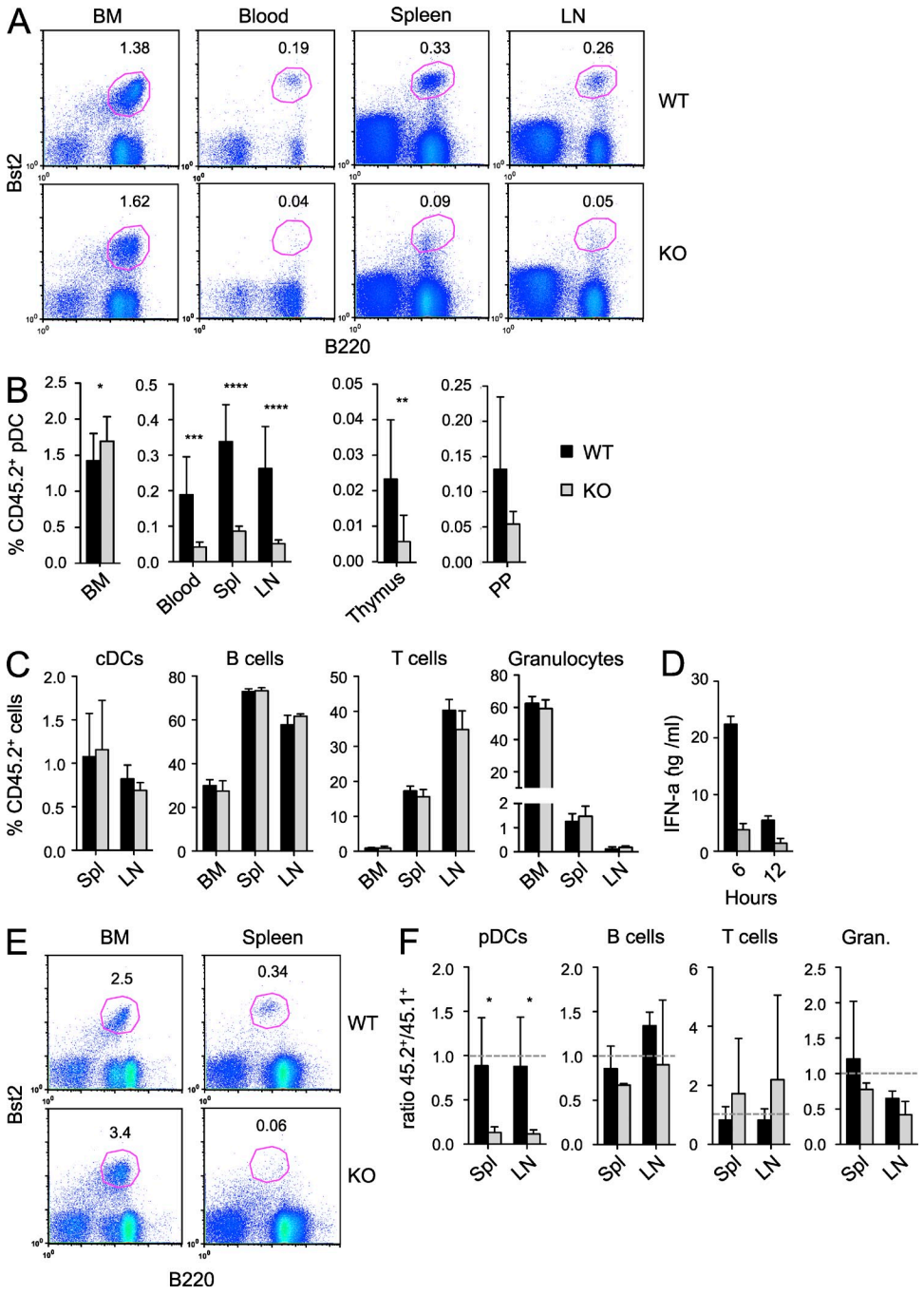

Figure 2. Loss of Runx2 leads to a specific decrease in peripheral pDCs. Recipient CD45.1$^+$ mice were reconstituted with *Runx2*$^{+/+}$ WT or *Runx2*$^{LacZ/LacZ}$ KO fetal liver cells alone (A–D) or in competition with CD45.1$^+$ BM cells (E and F). (A) Representative flow cytometric plots of donor-derived CD45.2$^+$ CD11b$^-$ cells from the indicated organs of recipient mice, with the Bst2$^+$ B220$^+$ pDC population highlighted in the gate. (B) The fraction of pDCs among total donor-derived cells was determined in the indicated organs (Spl, spleen; PP, Peyer's patches). Data represent mean ± SD; n = 18–19 mice/group for BM, spleen, and LN (three independent reconstitution experiments); n = 12 mice/group for blood (2 independent reconstitution experiments); n = 6–7 mice/group for thymus and PP (one reconstitution experiment). *, P < 0.05; **, P < 0.01; ***, P < 0.001; ****, P < 0.0001. (C) The fraction of cDCs (CD11c^{hi} MHC cl II$^+$), B cells (Bst2$^-$ B220$^+$), T cells (TCRβ$^+$), and granulocytes (SSC^{hi} Gr-1$^+$) was determined among total donor-derived cells in the indicated organs (mean ± SD of 12 mice per genotype, two independent reconstitution experiments). (D) WT and KO mice were injected with 5 µg CpG, and serum IFN-α was measured by ELISA 6 and 12 h later (mean ± SD of 5 recipient mice from one reconstitution, representative of two independent experiments). (E) The fraction of Bst2$^+$ B220$^+$ pDCs was determined among CD45.2$^+$ donor-derived cells in the BM or spleen of competitively reconstituted recipients (staining profiles representative of 5 recipient mice from one experiment). (F) Ratio of donor-derived CD45.2$^+$ to competitor-derived CD45.1$^+$ cells was determined within the indicated lineages. The CD45.2$^+$/CD45.1$^+$ ratios in the spleen and LN were normalized by the corresponding ratio in the BM, taken as 1 (dashed line). Bars represent mean ± SD of five mice per group from one experiment. *, P < 0.05.

at normal frequencies. These results confirm that the loss of peripheral pDCs after Runx2 deletion is cell intrinsic, consistent with the pDC-specific expression of Runx2.

No consistent increase in the fraction of Annexin V$^+$ pDCs was detected in the KO BM (unpublished data), arguing against pDC apoptosis as a primary cause of the phenotype. However, increased pDC fraction in the KO BM suggested retention of mature pDCs in the BM. Ly49Q is a pDC-specific receptor expressed on the majority of peripheral pDCs and on the subset of BM pDCs that corresponds to fully mature cells (Kamogawa-Schifter et al., 2005; Omatsu et al., 2005). We found that the fraction of Runx2-deficient Ly49Q$^+$ pDCs was significantly increased in the BM but drastically reduced in the periphery (Fig. 3, A and B). Indeed, the ratio of Ly49Q$^+$ to Ly49Q$^-$ cells was significantly increased (~1.5-fold) among KO pDCs in the BM, but reduced 5–6-fold in the periphery (Fig. 3 C). The residual Ly49Q$^-$ pDCs in the periphery of KO chimeras likely arise from immature Ly49Q$^-$ BM pDCs, which may migrate from the BM with low efficiency by a Runx2-independent mechanism. This is consistent with the documented migration of immature Ccr9$^-$ pDCs to the periphery, where they can give rise to mature pDCs (Schlitzer et al., 2011). Collectively, these data suggest that Runx2-deficient mature pDCs accumulate in the BM and fail to migrate into the periphery, causing the overall depletion of pDCs.

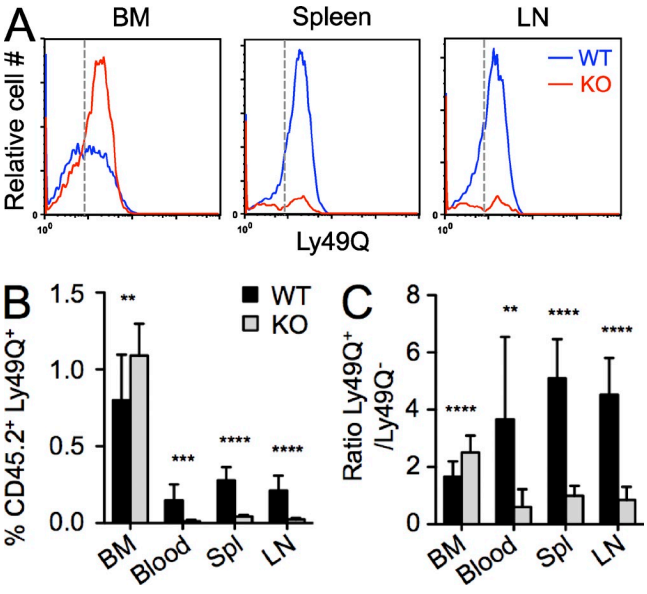

Figure 3. Runx2 deletion affects the mature Ly49Q$^+$ fraction of pDCs. (A) The expression of Ly49Q was determined by flow cytometry on donor-derived pDCs of recipient mice reconstituted with WT or *Runx2*$^{LacZ/LacZ}$ KO fetal livers. Fluorescence histograms representing relative cell numbers were derived from gated CD45.2$^+$ CD11b$^-$ Bst2$^+$ B220$^+$ pDCs in the indicated organs. (B) The fraction of Ly49Q$^+$ pDCs among total donor-derived cells was determined in the indicated organs of recipient mice. The group numbers and significance are as in Fig. 2 B. (C) The ratio of Ly49Q$^+$ to Ly49Q$^-$ pDC subsets was determined in the indicated organs of recipient mice analyzed in B.

Runx2 regulates a distinct subset of pDC-enriched genes

To explore the mechanism of Runx2 activity in pDCs, we performed genome-wide expression analysis of donor-derived WT or KO pDCs sorted from the BM of recipient mice (Supplemental Dataset 1). Pairwise comparison of expression profiles revealed small subsets of genes whose expression differed >2-fold between WT and KO pDCs (Fig. 4 A). Several of these differentially expressed genes encoded surface markers, allowing validation by single-cell analysis. In particular, the expression of CD11c was reduced, whereas the expression of CD8α and c-Kit was increased on KO pDCs (Fig. 4 B). We further examined the genes that are enriched in the pDC lineage compared with cDCs (the "pDC signature" genes; Elpek et al., 2011). Whereas the majority of these signature genes were unchanged, a small set of genes (36 out of 872, 4.1%) were reduced in KO pDCs (Fig. 4 C). Thus, Runx2 regulates a distinct subset of the pDC-specific gene expression program.

The genes down-regulated in Runx2-deficient pDCs included *Ccr2* and *Ccr5*, two related chemokine receptors that are preferentially expressed in pDCs compared with cDCs (Elpek et al., 2011). Because Ccr2 and Ccr5 are known regulators of immune cell migration, we focused on their potential role in pDCs downstream of Runx2. Reduced expression of both *Ccr2* (~2-fold) and *Ccr5* (~5-fold) transcripts in KO pDCs was confirmed by qRT-PCR (Fig. 4 D). We next measured the ability of pDCs to migrate in vitro to chemokines MCP-1 (Ccr2 ligand) as well as MIP-1α and RANTES (Ccr5 ligands) in a trans-well assay. The percentage of migrating cells in response to each of these chemokines was reduced in Runx2-deficient KO pDCs (Fig. 4 E). Thus, Runx2 facilitates the functional expression of Ccr2 and Ccr5 in the pDCs.

Ccr5 facilitates the migration of pDCs to the periphery

To explore the role of Ccr2 and Ccr5 in the steady-state migration of pDCs, we tested their expression at the surface of pDCs. Ccr2 was expressed only in a fraction of pDCs in the BM and periphery, whereas Ccr5 was expressed prominently in nearly all pDCs (Fig. 5 A). The expression of both receptors was up-regulated in the mature Ly49Q$^+$ pDCs compared with immature Ly49Q$^-$ pDCs in the BM (Fig. 5 B). The surface levels of both Ccr2 and Ccr5 were strongly reduced in Runx2-deficient pDCs, particularly in the Ly49Q$^+$ subset (Fig. 5 C). These results suggest that the expression of Ccr2 and Ccr5 is induced on pDCs in a Runx2-dependent manner during their maturation in the BM.

Ccr2 and Ccr5 are encoded by closely adjacent homologous genes and may show genetic redundancy. We found that the fraction of Ccr2$^+$ cells was increased in *Ccr5*$^{-/-}$ pDCs (Fig. 5 D), suggesting that Ccr5 deficiency causes a compensatory up-regulation of Ccr2. In contrast, the expression of Ccr5 was not changed in *Ccr2*$^{-/-}$ animals. The heterogeneous Ccr2 expression on pDCs argues against a primary role of this receptor in pDC migration. Indeed, the analysis of pDC populations in competitively reconstituted recipients of *Ccr2*$^{-/-}$ BM (Yona et al., 2013) did not reveal any cell-intrinsic defects (data not shown). On the other hand, the prominent homogeneous

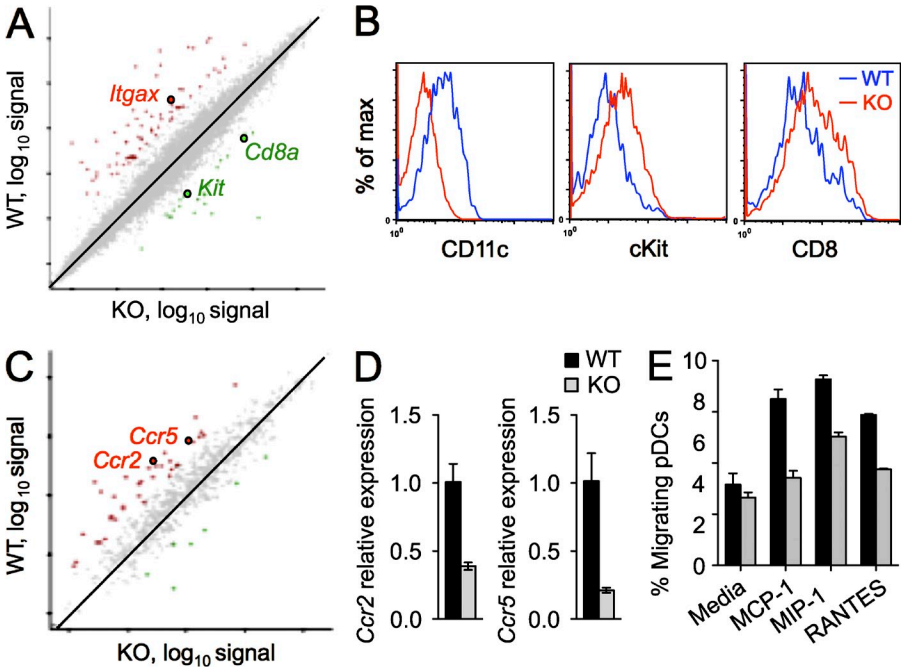

Figure 4. Runx2 regulates a subset of pDC-enriched genes. (A) pDCs were sorted from the pooled BM of recipient mice reconstituted with WT or *Runx2*$^{LacZ/LacZ}$ (KO) fetal livers. Genome-wide expression profiles of WT and KO pDCs were analyzed by microarray and plotted as pairwise comparison of total microarray probe signals. The probes with greater than twofold increased or decreased expression in KO pDCs were shown in green and red, respectively; the probes for select genes encoding surface markers were highlighted. (B) pDCs from the BM of WT or KO recipient mice were analyzed by flow cytometry for the expression of surface markers whose transcript levels were changed in the microarray data (A). Data are representative of two independent experiments. (C) Microarray probe signals corresponding to the pDC signature gene set (Elpek et al., 2011) were compared between WT and KO pDCs as in A. Probes for the genes encoding chemokine receptors Ccr2 and Ccr5 were highlighted. (D) The expression of Ccr2 and Ccr5 transcripts in donor-derived pDCs from the BM of WT or KO recipient mice was determined by qRT-PCR. Data represent mean ± SD of triplicate PCR reactions, derived from a single pair of pDC samples distinct from those used for microarray analysis. (E) pDC-enriched fractions of the BM from WT or KO recipient mice were tested in a trans-well assay for migration to chemokines MCP-1 (Ccr2 ligand) and MIP-1α and RANTES (Ccr5 ligands). The percentages of donor-derived pDCs migrating in response to the indicated chemokines were determined by flow cytometry (mean ± SD of duplicate cultures; representative of two independent experiments).

expression of Ccr5 and the apparent compensatory changes in *Ccr5*$^{-/-}$ pDCs suggested a role of Ccr5 in pDC migration.

The analysis of *Ccr5*$^{-/-}$ animals revealed normal pDC numbers in the BM and spleen, but a twofold decrease in the number of pDCs in the LN (unpublished data). To confirm the cell-intrinsic role of Ccr5 in pDC migration, we performed competitive reconstitution by mixing equal numbers of *Ccr5*$^{-/-}$ (CD45.2$^+$) and WT (CD45.1$^+$) BM cells and transplanting them into irradiated WT recipients (CD45.1$^+$). To reduce the likely compensatory effects of Ccr2, we also transplanted the same BM mixture into the recipients deficient in MCP-1 (Ccl2), one of the two major Ccr2 ligands (Jia et al., 2008; Tsou et al., 2007). B cells do not express Ccr5 (unpublished data), and the fraction of *Ccr5*$^{-/-}$ B cells was similar between the BM, spleen, and LN in all recipients. In contrast, the fraction of total *Ccr5*$^{-/-}$ pDCs was increased in the BM of WT recipients (Fig. 5 E). When normalized by B cells, the fraction of Ccr5-deficient mature Ly49Q$^+$ pDCs was significantly higher in the BM compared with LN in all recipients (Fig. 5 F). Notably, MCP-1–deficient recipients showed a significant progressive reduction of Ly49Q$^+$ pDCs in the spleen and LN compared with the BM (Fig. 5 F). These data suggest that Ccr5 contributes to the migration of pDCs from the BM to the spleen and especially to the LN, and its function can be partially substituted by Ccr2.

Our data demonstrate that, within the murine hematopoietic system, Runx2 is expressed exclusively in the pDC lineage. Consistent with its activation by the pDC master regulator E2-2, Runx2 is dispensable for pDC lineage commitment but regulates late steps of pDC differentiation. This includes the acquisition of pDC-related surface markers (such as the expression of DC marker CD11c) and migration from the BM into the periphery. The documented expression of human *RUNX2* in normal and malignant pDCs (Dijkman et al., 2007; Crozat et al., 2010) suggests that its function in this lineage is evolutionarily conserved. Our results reveal the complexity of the pDC-specific transcriptional network, whose members govern successive differentiation steps, including commitment and maintenance (E2-2), maturation within the BM (SpiB) and migration to the periphery (Runx2). In addition, they establish Runx2 as one of the few regulators of immune system development that are highly lineage-specific in their expression and function. Finally, these results show that the entire Runx protein family, including Runx2, has important functions in immune system development.

Unlike many cell types, including T and B lymphocytes and cDCs, pDCs develop to full functional maturity in the BM. Thus, the migration from the BM to the periphery represents a distinct checkpoint of pDC development, and here we identify Runx2 as its key regulator. The function of Runx2 is likely mediated through multiple target genes, which collectively facilitate pDC migration. For instance, Runx2-deficient pDCs showed low levels of CD11c, an integrin whose function is unknown but likely involves migration control. In addition, our results implicate chemokine receptor Ccr5 as a target of Runx2 that controls pDC migration into the periphery. Ccr5 facilitates the migration of multiple cell types, including activated pDCs into LN (Diacovo et al., 2005);

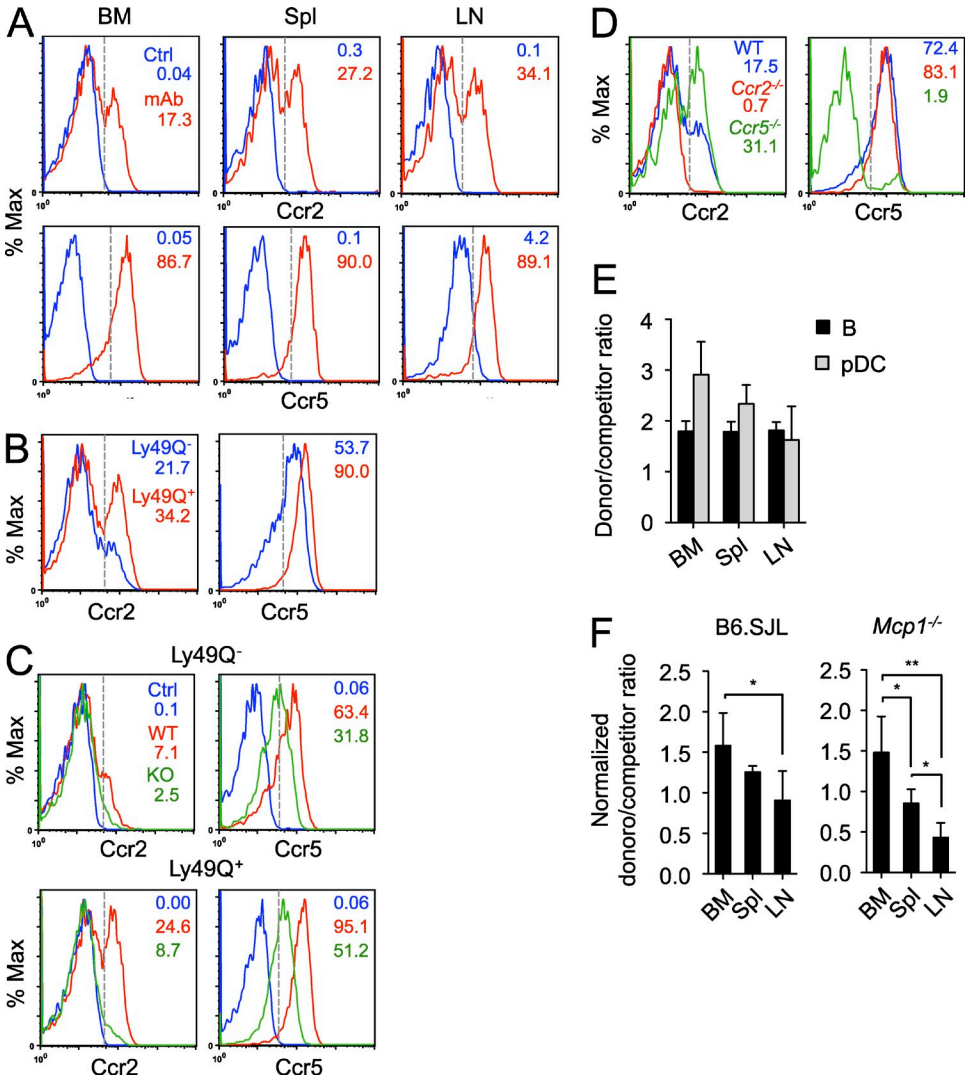

Figure 5. Ccr5 facilitates the migration of pDCs to the periphery. In A–C, surface expression of Ccr2 and Ccr5 was determined by flow cytometry on gated pDCs from recipient mice reconstituted with WT or *Runx2*$^{LacZ/LacZ}$ (KO) fetal livers. The fractions of Ccr2$^-$ or Ccr5$^+$ cells relative to isotype control (Ctrl) staining of WT cells (dashed line) were determined. Data represent mean positive cell fractions derived from six recipient mice per group in a single reconstitution experiment. (A) The expression of Ccr2 and Ccr5 on donor-derived pDCs was determined in WT recipients. (B) The expression of Ccr2 and Ccr5 in the Ly49Q$^-$ and Ly49Q$^+$ fractions of BM pDCs was determined in WT recipients. (C) The expression of Ccr2 and Ccr5 in the donor-derived BM pDCs was determined in WT and KO recipients. (D) Surface expression of Ccr2 and Ccr5 was determined as in A and B on pDCs from the BM of WT, *Ccr2*$^{-/-}$, and *Ccr5*$^{-/-}$ animals. Representative of two individual mice per genotype. In E and F, BM cells from *Ccr5*$^{-/-}$ (CD45.2$^+$) and WT (B6.SJL, CD45.1$^+$) mice were mixed 1:1 and transplanted into irradiated WT (B6.SJL) or MCP-1–deficient (*Mcp1*$^{-/-}$) recipients. Recipient mice were analyzed by flow cytometry 6 wk later; data represent mean ± SD of 4 recipient mice of each type from a single reconstitution. (E) The ratio of Ccr5-deficient donor to WT competitor cells was determined among B cells and total pDCs in WT recipients. (F) The donor/competitor ratio among Ly49Q$^+$ pDCs was determined and normalized to that in B cells in WT and MCP-1–deficient recipients. *, $P < 0.05$; **, $P < 0.01$.

however, its expression and role in the steady-state pDCs have not been explored previously. The function of Ccr5 in pDCs appears to be partially redundant with Ccr2, whose expression is increased on Ccr5-deficient pDCs. The combined loss of Ccr5 and one Ccr2 ligand (MCP-1) revealed a cell-intrinsic role of Ccr5 in pDC migration from the BM to the spleen and particularly to the LN. However, MCP-1 is partially redundant with MCP-3 (Tsou et al., 2007; Jia et al., 2008), thus the complete loss of Ccr5 and Ccr2 signaling is likely to cause stronger impairment of pDC migration. Although the Ccr2/Ccr5 double-deficient animals are currently unavailable, this possibility could be tested in the future. Importantly, our results suggest that pDC migration may be affected by pharmacological inhibition of Ccr5 and/or Ccr2. This possibility and its implications for pDC function should be considered in designing and interpreting the applications of Ccr5/Ccr2 inhibitors.

MATERIALS AND METHODS

Animals. All experiments were performed according to the investigator's protocol approved by the Institutional Animal Care and Use Committee of Columbia University. *Runx2*^{LacZ} mice (Otto et al., 1997; provided by

G. Karsenty and S. Kousteny, Columbia University, New York, NY) were backcrossed to C57BL/6 background for >10 generations. Animals deficient for Ccr5, Ccr2, and Ccl2 (C57BL/6 background) were obtained from The Jackson Laboratory. For hematopoietic reconstitution, *Runx2*$^{LacZ/+}$ mice were intercrossed and embryos isolated on day 14.5 post-coitum and genotyped. Fetal liver cells (2×10^6) from *Runx2*$^{LacZ/LacZ}$ or littermate control *Runx2*$^{+/+}$ embryos were injected i.v. into lethally irradiated C57BL/6 mice congenic for CD45.1 (B6.SJL; Taconic). Donor reconstitution reached >90% in all recipients. For competitive reconstitution, 10^6 fetal liver cells were mixed with 10^6 BM cells from B6.SJL mice and transplanted as above. For the analysis of Ccr5 function, BM cells from *Ccr5*$^{-/-}$ and B6.SJL mice were mixed 1:1 and transplanted (2×10^6/recipient) into irradiated B6.SJL (CD45.1$^+$) or *Ccl2*$^{-/-}$ (CD45.2$^+$) mice. The fraction of *Ccr5*$^{-/-}$ (CD45.2$^+$) cells was similar in both recipient groups, suggesting a nearly complete reconstitution by donor cells. All recipients were analyzed at least 2 mo after reconstitution. For in vivo IFN-I response, mice were injected i.v. with 5 µg CpG (ODN 2216; InvivoGen) complexed with DOTAP (Roche), and serum IFN-α production was measured by ELISA (PBL Interferon Source).

Cell analysis. Flow cytometric analysis and sorting were performed as previously described (Cisse et al., 2008). The expression of LacZ was measured with the fluorescent LacZ substrate fluorescein di-β-D-galactopyranoside using the FluoReporter LacZ Flow Cytometry kit (Invitrogen). The expression of Ccr2 and Ccr5 was detected with mAb MC-21 and MC-68, respectively (Mack et al., 2001). The cells were stained with these mAb (rat IgG2b) or an isotype control, followed by biotin-conjugated mouse anti-rat IgG2b (BD Biosciences); blocked in 10% rat serum; and then stained with PerCP-Cy5.5-conjugated streptavidin and fluorophore-conjugated mAb to other surface markers.

For the migration assay, total BM cells from recipients of WT or KO fetal livers were depleted of lineage-positive cells (CD3, Ter119, CD19, NK1.1, and Gr1) by magnetic cell separation (Miltenyi Biotec). Media containing 10 µg/ml of recombinant MCP-1, MIP1-α, or RANTES (PeproTech) was added to the well and 2×10^5 enriched cells were placed in the trans-well insert with 5-µm pore size (Corning). After 3-h incubation at 37°C, cells that had passed through the trans-well insert were collected and the number of pDCs was measured by flow cytometry.

ChIP-Seq analysis and shRNA-mediated knockdown of E2-2 in human pDC cell lines CAL-1 (Maeda et al., 2005) and Gen2.2 (Chaperot et al., 2006) will be described in a separate publication. In brief, ChIP-Seq in CAL-1 cells was performed using a newly developed rabbit mAb to E2-2, and E2-2-bound or total input chromatin were amplified and sequenced on a HiSeq 2000 instrument (Illumina). Sequencing reads were aligned to the human genome (UCSC hg19), and binding peaks were visualized using DNANexus genome browser (DnaNexus, Inc). For inducible knockdown, CAL-1 and Gen2.2 were retrofitted with ecotropic retrovirus receptor and tetracycline repressor for Dox-inducible retroviral expression of shRNAs (Ngo et al., 2006). Cells were transduced with pRSMX vector-based constructs expressing E2-2–specific shRNA under tetracycline-inducible promoter, selected with puromycin and split into parallel cultures with or without 0.5 mg/ml Dox.

Gene expression analysis. For microarray analysis, BM cells from recipients of WT or KO fetal livers were pooled and depleted of lineage-positive cells using magnetic cell separation. Donor-derived pDCs (CD45.2$^+$ CD11b$^-$ B220$^+$ Bst2$^+$) were sorted directly into TRIzol reagent (Invitrogen), and total RNA was reverse transcribed, amplified, labeled, and hybridized to Mouse Genome 1.0 ST arrays (Affymetrix). The results were gcRMA-normalized by the manufacturer's software and filtered by matching to the probeset used by ImmGen consortium (Crozat et al., 2010; Satpathy et al., 2011; Miller et al., 2012). Pairwise analysis was performed using the NIA Array software. RNA from a separately sorted pDC sample was reverse transcribed and assayed by qRT-PCR for the indicated genes as previously described (Cisse et al., 2008). All microarray data are deposited in the NCBI's GEO database under the accession no. GSE49859.

Statistical analyses. All p-values were calculated by unpaired, two-tailed Student's *t* test.

Online supplemental material. A supplemental dataset contains the microarray probes. Online supplemental material is available at http://www.jem.org/cgi/content/full/jem.20130443/DC1.

We thank D. Rashkovan and S. Jung for analyzing *Ccr2*$^{-/-}$ chimeric mice, M. Mack for antibodies to Ccr2 and Ccr5, G. Karsenty and S. Kousteny for the *Runx2*^{LacZ} strain, J. Plumas and L. Chaperot for Gen2.2 cells, D. Ganguly for control qPCR, and Y. Goltsev for helpful discussions.

This work was supported by the New York State Department of Health grant N09G-22, National Institutes of Health grant AI072571, and Leona M. and Harry B. Helmsley Charitable Trust (B. Reizis), Irvington Institute Fellowship of the Cancer Research Institute (V. Sisirak), and American Society of Hematology (H.S. Ghosh).

The authors declare no competing financial interests.

Submitted: 1 March 2013
Accepted: 10 September 2013

REFERENCES

Asselin-Paturel, C., G. Brizard, K. Chemin, A. Boonstra, A. O'Garra, A. Vicari, and G. Trinchieri. 2005. Type I interferon dependence of plasmacytoid dendritic cell activation and migration. *J. Exp. Med.* 201:1157–1167. http://dx.doi.org/10.1084/jem.20041930

Bao, M., and Y.J. Liu. 2013. Regulation of TLR7/9 signaling in plasmacytoid dendritic cells. *Protein Cell.* 4:40–52. http://dx.doi.org/10.1007/s13238-012-2104-8

Cervantes-Barragan, L., K.L. Lewis, S. Firner, V. Thiel, S. Hugues, W. Reith, B. Ludewig, and B. Reizis. 2012. Plasmacytoid dendritic cells control T-cell response to chronic viral infection. *Proc. Natl. Acad. Sci. USA.* 109:3012–3017. http://dx.doi.org/10.1073/pnas.1117359109

Chaperot, L., A. Blum, O. Manches, G. Lui, J. Angel, J.P. Molens, and J. Plumas. 2006. Virus or TLR agonists induce TRAIL-mediated cytotoxic activity of plasmacytoid dendritic cells. *J. Immunol.* 176:248–255.

Cisse, B., M.L. Caton, M. Lehner, T. Maeda, S. Scheu, R. Locksley, D. Holmberg, C. Zweier, N.S. den Hollander, S.G. Kant, et al. 2008. Transcription factor E2-2 is an essential and specific regulator of plasmacytoid dendritic cell development. *Cell.* 135:37–48. http://dx.doi.org/10.1016/j.cell.2008.09.016

Collins, A., D.R. Littman, and I. Taniuchi. 2009. RUNX proteins in transcription factor networks that regulate T-cell lineage choice. *Nat. Rev. Immunol.* 9:106–115. http://dx.doi.org/10.1038/nri2489

Colonna, M., G. Trinchieri, and Y.J. Liu. 2004. Plasmacytoid dendritic cells in immunity. *Nat. Immunol.* 5:1219–1226. http://dx.doi.org/10.1038/ni1141

Crozat, K., R. Guiton, M. Guilliams, S. Henri, T. Baranek, I. Schwartz-Cornil, B. Malissen, and M. Dalod. 2010. Comparative genomics as a tool to reveal functional equivalences between human and mouse dendritic cell subsets. *Immunol. Rev.* 234:177–198. http://dx.doi.org/10.1111/j.0105-2896.2009.00868.x

Diacovo, T.G., A.L. Blasius, T.W. Mak, M. Cella, and M. Colonna. 2005. Adhesive mechanisms governing interferon-producing cell recruitment into lymph nodes. *J. Exp. Med.* 202:687–696. http://dx.doi.org/10.1084/jem.20051035

Dijkman, R., R. van Doorn, K. Szuhai, R. Willemze, M.H. Vermeer, and C.P. Tensen. 2007. Gene-expression profiling and array-based CGH classify CD4+CD56+ hematodermic neoplasm and cutaneous myelomonocytic leukemia as distinct disease entities. *Blood.* 109:1720–1727. http://dx.doi.org/10.1182/blood-2006-04-018143

Elpek, K.G., A. Bellemare-Pelletier, D. Malhotra, E.D. Reynoso, V. Lukacs-Kornek, R.H. DeKruyff, and S.J. Turley. 2011. Lymphoid organ-resident dendritic cells exhibit unique transcriptional fingerprints based on subset and site. *PLoS ONE.* 6:e23921. http://dx.doi.org/10.1371/journal.pone.0023921

Ghosh, H.S., B. Cisse, A. Bunin, K.L. Lewis, and B. Reizis. 2010. Continuous expression of the transcription factor e2-2 maintains the cell fate of mature plasmacytoid dendritic cells. *Immunity.* 33:905–916. http://dx.doi.org/10.1016/j.immuni.2010.11.023

Jia, T., N.V. Serbina, K. Brandl, M.X. Zhong, I.M. Leiner, I.F. Charo, and E.G. Pamer. 2008. Additive roles for MCP-1 and MCP-3 in CCR2-mediated

recruitment of inflammatory monocytes during Listeria monocytogenes infection. *J. Immunol.* 180:6846–6853.

Kamogawa-Schifter, Y., J. Ohkawa, S. Namiki, N. Arai, K. Arai, and Y. Liu. 2005. Ly49Q defines 2 pDC subsets in mice. *Blood*. 105:2787–2792. http://dx.doi.org/10.1182/blood-2004-09-3388

Li, H.S., A. Gelbard, G.J. Martinez, E. Esashi, H. Zhang, H. Nguyen-Jackson, Y.J. Liu, W.W. Overwijk, and S.S. Watowich. 2011. Cell-intrinsic role for IFN-α-STAT1 signals in regulating murine Peyer patch plasmacytoid dendritic cells and conditioning an inflammatory response. *Blood*. 118: 3879–3889. http://dx.doi.org/10.1182/blood-2011-04-349761

Liu, K., and M.C. Nussenzweig. 2010. Origin and development of dendritic cells. *Immunol. Rev.* 234:45–54. http://dx.doi.org/10.1111/j.0105-2896.2009.00879.x

Long, F. 2012. Building strong bones: molecular regulation of the osteoblast lineage. *Nat. Rev. Mol. Cell Biol.* 13:27–38. http://dx.doi.org/10.1038/nrm3254

Mack, M., J. Cihak, C. Simonis, B. Luckow, A.E. Proudfoot, J. Plachý, H. Brühl, M. Frink, H.J. Anders, V. Vielhauer, et al. 2001. Expression and characterization of the chemokine receptors CCR2 and CCR5 in mice. *J. Immunol.* 166:4697–4704.

Maeda, T., K. Murata, T. Fukushima, K. Sugahara, K. Tsuruda, M. Anami, Y. Onimaru, K. Tsukasaki, M. Tomonaga, R. Moriuchi, et al. 2005. A novel plasmacytoid dendritic cell line, CAL-1, established from a patient with blastic natural killer cell lymphoma. *Int. J. Hematol.* 81:148–154. http://dx.doi.org/10.1532/IJH97.04116

Miller, J.C., B.D. Brown, T. Shay, E.L. Gautier, V. Jojic, A. Cohain, G. Pandey, M. Leboeuf, K.G. Elpek, J. Helft, et al; Immunological Genome Consortium. 2012. Deciphering the transcriptional network of the dendritic cell lineage. *Nat. Immunol.* 13:888–899. http://dx.doi.org/10.1038/ni.2370

Ngo, V.N., R.E. Davis, L. Lamy, X. Yu, H. Zhao, G. Lenz, L.T. Lam, S. Dave, L. Yang, J. Powell, and L.M. Staudt. 2006. A loss-of-function RNA interference screen for molecular targets in cancer. *Nature*. 441:106–110. http://dx.doi.org/10.1038/nature04687

Omatsu, Y., T. Iyoda, Y. Kimura, A. Maki, M. Ishimori, N. Toyama-Sorimachi, and K. Inaba. 2005. Development of murine plasmacytoid dendritic cells defined by increased expression of an inhibitory NK receptor, Ly49Q. *J. Immunol.* 174:6657–6662.

Otto, F., A.P. Thornell, T. Crompton, A. Denzel, K.C. Gilmour, I.R. Rosewell, G.W. Stamp, R.S. Beddington, S. Mundlos, B.R. Olsen, et al. 1997. Cbfa1, a candidate gene for cleidocranial dysplasia syndrome, is essential for osteoblast differentiation and bone development. *Cell*. 89:765–771. http://dx.doi.org/10.1016/S0092-8674(00)80259-7

Reizis, B., A. Bunin, H.S. Ghosh, K.L. Lewis, and V. Sisirak. 2011. Plasmacytoid dendritic cells: recent progress and open questions. *Annu. Rev. Immunol.* 29:163–183. http://dx.doi.org/10.1146/annurev-immunol-031210-101345

Sasaki, I., K. Hoshino, T. Sugiyama, C. Yamazaki, T. Yano, A. Iizuka, H. Hemmi, T. Tanaka, M. Saito, M. Sugiyama, et al. 2012. Spi-B is critical for plasmacytoid dendritic cell function and development. *Blood*. 120:4733–4743. http://dx.doi.org/10.1182/blood-2012-06-436527

Satpathy, A.T., K.M. Murphy, and W. Kc. 2011. Transcription factor networks in dendritic cell development. *Semin. Immunol.* 23:388–397. http://dx.doi.org/10.1016/j.smim.2011.08.009

Schlitzer, A., J. Loschko, K. Mair, R. Vogelmann, L. Henkel, H. Einwächter, M. Schiemann, J.H. Niess, W. Reindl, and A. Krug. 2011. Identification of CCR9$^-$ murine plasmacytoid DC precursors with plasticity to differentiate into conventional DCs. *Blood*. 117:6562–6570. http://dx.doi.org/10.1182/blood-2010-12-326678

Seth, S., L. Oberdörfer, R. Hyde, K. Hoff, V. Thies, T. Worbs, S. Schmitz, and R. Förster. 2011. CCR7 essentially contributes to the homing of plasmacytoid dendritic cells to lymph nodes under steady-state as well as inflammatory conditions. *J. Immunol.* 186:3364–3372. http://dx.doi.org/10.4049/jimmunol.1002598

Swiecki, M., S. Gilfillan, W. Vermi, Y. Wang, and M. Colonna. 2010. Plasmacytoid dendritic cell ablation impacts early interferon responses and antiviral NK and CD8(+) T cell accrual. *Immunity*. 33:955–966. http://dx.doi.org/10.1016/j.immuni.2010.11.020

Tai, L.H., M.L. Goulet, S. Belanger, N. Toyama-Sorimachi, N. Fodil-Cornu, S.M. Vidal, A.D. Troke, D.W. McVicar, and A.P. Makrigiannis. 2008. Positive regulation of plasmacytoid dendritic cell function via Ly49Q recognition of class I MHC. *J. Exp. Med.* 205:3187–3199. http://dx.doi.org/10.1084/jem.20080718

Tsou, C.L., W. Peters, Y. Si, S. Slaymaker, A.M. Aslanian, S.P. Weisberg, M. Mack, and I.F. Charo. 2007. Critical roles for CCR2 and MCP-3 in monocyte mobilization from bone marrow and recruitment to inflammatory sites. *J. Clin. Invest.* 117:902–909. http://dx.doi.org/10.1172/JCI29919

Wendland, M., N. Czeloth, N. Mach, B. Malissen, E. Kremmer, O. Pabst, and R. Förster. 2007. CCR9 is a homing receptor for plasmacytoid dendritic cells to the small intestine. *Proc. Natl. Acad. Sci. USA*. 104:6347–6352. http://dx.doi.org/10.1073/pnas.0609180104

Yona, S., K.W. Kim, Y. Wolf, A. Mildner, D. Varol, M. Breker, D. Strauss-Ayali, S. Viukov, M. Guilliams, A. Misharin, et al. 2013. Fate mapping reveals origins and dynamics of monocytes and tissue macrophages under homeostasis. *Immunity*. 38:79–91. http://dx.doi.org/10.1016/j.immuni.2012.12.001